第10卷第2期2012年6月
1672-6553/2012/10(2)/171-6
动力学与控制学报
JOURNAL OF DYNAMICS AND CONTROL
Vol. 10 No. 2
Jun. 2012

风力机叶片大挠度挥舞振动特性分析*

刘启宽[1,3]　李亮[2]　张志军[3]　李映辉[2]
(1. 昆明学院数学系,昆明　650214)(2. 西南交通大学力学与工程学院,成都　610031)
(3. 成都信息工程学院数学学院,成都　610225)

摘要　分析了风力机叶片大挠度挥舞振动特性. 基于Hamilton原理,建立了叶片大挠度挥舞振动控制方程,其中非稳态气动力由Greenberg公式得出. 使用瑞利-利兹法求解振动特征问题,得到振动的频率和无阻尼模态函数. 基于得出的模态函数,使用Galerkin方法将控制偏微分方程离散,得到模态坐标方程. 将振动位移分解为静态位移和动态位移,得到了静态位移和动态位移方程,考查了入流速度比对静态位移和气动阻尼的影响,并对大挠度挥舞振动动态响应进行了分析,得到如下结论:大挠度挥舞振动静态位移沿叶片展向随入流速度比的增大而增大,叶尖处位移最大;当入流速度比较小时,振动为小振幅的周期运动,入流速度比较大时,振动为大振幅的拟周期运动.

关键词　风力机叶片,　大挠度,　挥舞振动

引言

风力机叶片有挥舞、摆振、扭转三种振动形式. 对于叶片振动特性的研究,李本立等[1]使用矩阵分析法讨论了叶片扭转角、轮毂、变距机构对不旋转叶片固有频率的影响,以及转速对旋转叶片固有频率的影响. Mahri[2-4]建立了叶片挥舞振动的悬臂梁模型,使用有限元计算了挥舞振动的前三阶频率和模态,并进行了疲劳分析. Song和Librescu[5]建立了尖部带集中质量的叶片挥舞-摆振耦合模型,并讨论了叶片转速和集中质量对前三阶挥舞振动频率和模态的影响. 韩新月等[6]基于叶素理论和风力机理论,建立了叶片科氏加速度理论计算模型,给出了考虑科氏力时风力机叶片频率的计算方法,研究了科氏力对挥舞、摆振、扭转频率的影响. 吕计男与刘子强[7]使用有限元建立了NRELS809双叶片风力机复合材料叶片实体模型,分析了旋转软化和动力刚化效应对叶片固有模态的影响. 王建礼等[8]基于有限元方法,开发了风力机叶片固有频率计算程序,通过优化叶片梁帽质量分布来优化固有频率. 梁明轩和陈长征[9]讨论了流固耦合效应对叶片模态特性的影响. 李静等[10]使用瑞利能量法得到了叶片固有频率方程,讨论了转速和叶片长度对挥舞频率的影响. Larsen等[11-13]使用有限元方法建立了叶片挥舞-摆振-扭转耦合模型,研究了挥舞-摆振的1:2内共振、一般情况下的参数不稳定性和随机稳定性. 现有研究大多使用有限元方法分析振动特性,近似方法使用的相对较少. 此外,分叉、庞加莱映射、相图、时间历程图等非线性动力学工具也未用于叶片振动的研究. 研究内容方面,风速对于阻尼和静态位移的具体影响还尚未有人研究.

风力机叶片结构复杂,截面弯曲刚度和质量随展向变化,计算固有频率时还需要考虑俯仰角、安装角、截面扭转角等参数的影响. 若使用有限元计算,几何模型建立非常困难,另外计算也较费时. 本文将使用哈密顿原理建立叶片大挠度挥舞振动控制方程,采用瑞利-利兹法计算叶片频率及模态函数,基于得出的模态函数使用非线性动力学工具对振动响应进行分析,并讨论风速对静态位移和阻尼的影响.

1　控制方程

如图1,$XYYZ$是风轮坐标系,原点在轮毂中心,OZ沿转轴方向,叶片与XY平面的夹角为锥角β_p,坐标系以角速度Ω绕Z轴转动;$O'xyz$是叶片坐

2011-10-09收到第1稿,2012-02-14收到修改稿.
*国家自然科学基金项目资助(11072204),四川省应用基础研究计划项目资助(2010JY0079),昆明学院引进人才科研项目资助(YJL12005)

标系,原点在叶片根部,x 轴沿弹性轴方向,y 轴沿摆振方向,z 轴沿挥舞振动方向;$O^{\xi}\eta\zeta$ 是叶片切面坐标系,原点在截面剪切中心,ξ 轴垂直于截面,η 轴沿弦线方向. 引用文献[1]中由格林伯格公式得出的气动力

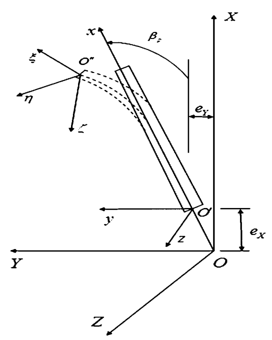

图1 坐标系

Fig. 1 Coordinate systems

$$F_x^A = 0 \tag{1}$$

$$F_z^A = (\rho ac/2)\Omega^2[(1-\beta)x^2\sin\theta + 2e_X x\sin\theta - \lambda R(x+e_X)\cos\theta - e_Y\beta_p x] + (\rho ac/2)\Omega^2[(c/2 + (c/4)\cos\theta - e_A)(\beta_p x + xw_{,x} - e_Y xw_{,x}] - (\rho ac/2)\Omega^2[x(1+C_{DO}/a) + \lambda R\sin\theta)w_{,t}/\Omega + (cw_{,tt}/4)\cos\theta/\Omega^2] \tag{2}$$

$$M_y^A = 0 \tag{3}$$

其中 ρ 是空气密度,a 为截面升力曲线斜率,c 为弦长,θ 是 y 轴与弦线夹角,R 是叶片旋转半径,C_{DO} 为阻力系数,w 为挥舞位移,t 为时间,x 为叶片截面到叶根的距离,(e_x,e_y) 为偏置量 e 在 $O'-XY$ 下的坐标,e_A 是气动中心到弹性轴的距离,入流速度比 $\lambda(x,t) = \lambda_0 + \lambda_1(r_x/R)^2 + \lambda_2(r_x/R)\cos(\Omega t)$,$\lambda_0$ 是轮毂处的入流速度比,r_x 是叶片展长,,$\lambda_1 = [p(p-1)/4](R/h_0)^2(\lambda_0 + \sigma a/8)$,$p$ 是速度梯度常量,h_0 是轮毂高度,$\sigma = Nc/(\pi R)$ 是转子实度,N 是叶片数,$\lambda_2 = (-pR/h_0)(\lambda_0 + \sigma a/8)$.

令 I,J,K 为坐标系 $O-XYZ$ 的单位向量,任意横截面上的点 $P(x,y,z)$ 变形后的位置矢量可以表示为:

$$OP = [(x+e_x+u)\cos\beta_p - w\cos\theta\sin\beta_p - z\sin\beta_p]I + (y+e_Y - w\sin\theta)J + [(x-e_X+u)\sin\beta_p + (w\cos\theta + z)\cos\beta_p]K \tag{4}$$

这里 u 为轴向位移,点 P 的速度为:

$$v_P = [u_{,t}\cos\beta_p - w_{,t}\cos\theta\sin\beta_p - \Omega(e_Y - w\sin\theta) - \Omega y] + [\Omega(u+x+e_X)\cos\beta_p - \Omega(w\cos\theta + z)\sin\beta_p - w_{,t}\sin\theta]J + (u_{,t}\sin\beta_p + w_{,t}\cos\theta\cos\beta_p)K \tag{5}$$

则叶片动能 T 为:

$$T = \frac{1}{2}\int_0^L\int_A m(v_P\cdot v_P)\,\mathrm{d}A\mathrm{d}x \tag{6}$$

这里 L 是叶片总长,$m(x)$ 为单位长度的质量.

将叶片简化为 Bernoulli - Euler 梁,只考虑轴向正应变 ε_x,应变-位移关系为:

$$\varepsilon_x = u_{,x} - rw_{,xx} + (1/2)w_{,x}^2 \tag{7}$$

其中 r 是点到中性轴的距离. 则叶片势能 U 为:

$$U = \frac{1}{2}\int_0^L\int_A E\varepsilon_x^2\,\mathrm{d}A\mathrm{d}x \tag{8}$$

其中 E 为杨氏模量,$A(x)$ 为横截面积.

非保守力所作的虚功为:

$$\delta W(x,t) = F_x^A\delta u + F_z^A\delta w + M_y^A\delta w_{,x} \tag{9}$$

轴向拉力由离心力引起,即

$$F_T = \int_x^L m\Omega^2(e + y\cos\beta_p)\,\mathrm{d}y = EA(u_{,x} + w_{,x}^2/2) \tag{10}$$

可得

$$u_{,t} = -\int_0^x w_{,x}w_{,tx}\,\mathrm{d}x \tag{11}$$

由哈密顿原理,得叶片大挠度挥舞振动控制方程:

$$(EI\cos^2\theta w_{,xx})_{,xx} - (EAu_{,x}w_{,x})_{,x} - m\Omega^2(\sin^2\theta + \cos^2\theta\sin^2\beta_p)w + (m - \rho ac^2/8)w_{,tt} - (\rho ac/2)\Omega^2[c/2 + (c/4)\cos\theta - e_A - e_Y]xw_{,x} = -m\Omega^2 e_Y\sin\theta - m\Omega^2(x + e_X)\cos\theta\sin\beta_p\cos\beta_p - (\rho ac/2)\Omega^2\lambda R(x + e_X)\cos\theta\cos\beta_p + (\rho ac/2)\Omega^2[((1-\beta_p^2)x + 2e_X)x\sin\theta + (c/2 + (c/4)\cos\theta - e_A - e_Y)\beta_p x] + 2m\Omega\sin\theta\cos\beta_p u_{,t} - (\rho ac/2)\Omega^2(x - \lambda R\sin\theta)w_{,t} + (1/2)(EAw_{,x}^3) \tag{12}$$

边界条件为:

$$w|_{x=0} = 0,\quad w_{,x}|_{x=0} = 0,$$
$$(EIw)_{,xx}|_{x=L} = 0,\quad (EIw)_{,xxx}|_{x=L} = 0 \tag{13}$$

其中 $EI(x)$ 是挥舞弯曲刚度,$(EAu_{,x}w_{,x})_{,x}$ 和 $(EAw_{,x}^3/2)_{,x}$ 为几何非线性项,$2m\Omega\sin\theta\cos\beta_p u_{,t}$ 是科氏力,$(\rho ac/2)\Omega^2(x - \lambda R\sin\theta)w_{,t}$ 为气动阻尼,简谐激励由气动力提供,是 $(\rho ac/2)\Omega^2\lambda R(x + e_X)\cos\theta\cos\beta_p$ 中的时变部分. 由式(10)-(11),式(12)可化为

$$(EI\cos^2\theta w_{,xx})_{,xx} - (F_T w_{,x})_{,x} - m\Omega^2(\sin^2\theta +$$

$$\cos^2\theta\sin^2\beta_p)w + (m - \rho ac^2/8)w_{,tt} - (\rho ac/2)\Omega^2[c/2 + (c/4)\cos\theta - e_A - e_Y]xw_{,x} = -m\Omega^2 e_Y\sin\theta - m\Omega^2(x + e_X)\cos\theta\sin\beta_p\cos\beta_p - (\rho ac/2)\Omega^2\lambda R(x + e_X)\cos\theta\cos\beta_p + (\rho ac/2)\Omega^2[((1-\beta_p^2)x + 2e_X)x\sin\theta + (c/2 + (c/4)\cos\theta - e_A - e_Y)\beta_p x] - 2m\Omega\sin\theta\cos\beta_p\int_0^x w_{,x}w_{,tx}\mathrm{d}x - (\rho ac/2)\Omega(x - \lambda R\sin\theta)w_{,t} \tag{14}$$

2　振动特性分析

设
$$w = \gamma^{(w)}(x)e^{i\omega t} \tag{15}$$
得无阻尼模态的特征问题:
$$\frac{\mathrm{d}^2}{\mathrm{d}x^2}(EI\cos^2\theta\frac{\mathrm{d}^2\gamma^{(w)}}{\mathrm{d}x^2}) - \frac{\mathrm{d}^2}{\mathrm{d}x^2}(F_T\frac{\mathrm{d}\gamma^{(w)}}{\mathrm{d}x}) - m\Omega^2(\sin^2\theta + \cos^2\theta\sin^2\beta_p)\gamma^{(w)} - \frac{\rho ac\Omega}{2}(\frac{c}{2} + \frac{c}{4}\cos\theta - e_A - e_Y)x\frac{\mathrm{d}\gamma^{(w)}}{\mathrm{d}x} = (m - \rho ac^2/8)\omega^2\gamma^{(w)} \tag{16}$$
对式(16),瑞利商的平稳值
$$R(\gamma) = \frac{[\gamma,\gamma]}{(\sqrt{m - \frac{\rho ac^2}{8}}\gamma,\sqrt{m - \frac{\rho ac^2}{8}}\gamma)} \tag{17}$$
式中$[\gamma,\gamma]$为能量内积.

设
$$\gamma = \sum_{i=1}^n a_i\phi_i(x) \tag{18}$$
其中,a_i 为常数,$\phi_i(x)$为满足边界条件的试函数.
将式(18)代入式(17)得
$$R(a_1,a_2,\cdots,a_n) = \frac{[\sum_{i=1}^n[\sum_{i=1}^n a_i\phi_i(x),\sum_{i=1}^n a_i\phi_i(x)]}{(\sqrt{m - \frac{\rho ac^2}{8}}\sum_{i=1}^n a_i\phi_i(x),\sqrt{m - \frac{\rho ac^2}{8}}\sum_{i=1}^n a_i\phi_i(x))} = \frac{\sum_{i=1}^n\sum_{j=1}^n a_ia_j[\phi_i,\phi_j]}{\sum_{i=1}^n\sum_{j=1}^n a_ia_j(\sqrt{m - \frac{\rho ac^2}{8}}\phi_i,\sqrt{m - \frac{\rho ac^2}{8}}\phi_j)} \tag{19}$$
这里
$$[\phi_i,\phi_j]\int_0^L\sum_{k=0}^p a_k(L\phi_i)\phi_j\mathrm{d}x = k_{ij}, i,j = 1,2,\cdots,n \tag{20}$$
其中微分算子
$$L = \frac{\mathrm{d}^2}{\mathrm{d}x^2}(EI\cos^2\theta\frac{\mathrm{d}^2}{\mathrm{d}x^2}(\cdot)) - \frac{\mathrm{d}}{\mathrm{d}x}(F_T\cdot\frac{\mathrm{d}}{\mathrm{d}x}(\cdot)) + \frac{\rho ac\Omega^2}{2}[e_Yx - (c/2 + c\cos\theta/4 - e_A)x]\frac{\mathrm{d}}{\mathrm{d}x}(\cdot) - m\Omega^2(\sin^2\theta + \cos^2\theta\sin^2\beta_p)\cdot(\cdot)$$
$$(\sqrt{m - \frac{\rho ac^2}{8}}\phi_i,\sqrt{m - \frac{\rho ac^2}{8}}\phi_j) = \int_0^L(m - \frac{\rho ac^2}{8})\phi_i\phi_j\mathrm{d}x = m_{ij}, \quad i,j = 1,2,\cdots,n \tag{21}$$
将方程(20)、(21)代入方程(19),瑞利商可写成如下形式
$$R(a_1,a_2,\cdots,a_n) = \frac{N(a_1,a_2,\cdots,a_n)}{D(a_1,a_2,\cdots,a_n)} \tag{22}$$
式中,$N(a_1,a_2,\cdots,a_n) = \sum_{i=1}^n\sum_{j=1}^n k_{ij}a_ia_j, D(a_1,a_2,\cdots,a_n) = \sum_{i=1}^n\sum_{j=1}^n m_{ij}a_ia_j$.

使瑞利商平稳的条件为:
$$\frac{\partial R}{\partial a_s} = 0, \quad s = 1,2,\cdots,n \tag{23}$$
则应用到方程(22),得到
$$\frac{\partial R}{\partial a_s} = \frac{(\partial N/\partial a_s)D - (\partial D/\partial a_s)N}{D^2} = \frac{(\partial N/\partial a_s) - \omega(\partial D/\partial a_s)}{D} = 0, s = 1,2,\cdots,n \tag{24}$$
式中 ω—系统的特征值,瑞利商的平稳值恰好是系统的特征值.

而
$$\frac{\partial N}{\partial a_s} = 2\sum_{j=1}^n k_{sj}a_j, \frac{\partial D}{\partial a_s} = 2\sum_{j=1}^n k_{sj}a_j, \quad \frac{\partial D}{\partial a_s} = 2\sum_{j=1}^n m_{sj}a_j, \quad s = 1,2,\cdots,n \tag{25}$$
代入方程(24)得
$$\sum_{j=1}^n(k_{ij} - \omega m_{ij})a_j = 0, \quad i = 1,2,\cdots,n \tag{26}$$
其矩阵形式为
$$(K - \omega M)\{a_1,\cdots,a_n\}^T = 0 \tag{27}$$
因为 $a_1,\cdots,a_n$ 不全为零,所以由$|K - \omega M| = 0$ 可求得 ω 的值,记为:$\omega_1,\omega_2,\cdots,\omega_n$.

每个 $\omega_1,\omega_2,\cdots,\omega_n$ 对应的$\{a_1,\cdots,a_n\}^T$ 也可相应求出,进而可以得到模态 $\gamma_1,\gamma_2,\cdots,\gamma_n$.

3　响应分析

设
$$w = \sum_{k=1}^n\gamma_k(x)q_k(t) \tag{28}$$

其中 $\gamma_k(x)$ 是第 k 阶无阻尼模态,由 Galerkin 截断可得:

$$\ddot{q}_k + \omega_k^2 q_k = a_{s,k} - \sum_{i=1}^{n} c_{k,i}\dot{q}_i - \sum_{1\leqslant i,j\leqslant n} b_{k,ij} q_i \dot{q}_j + f_k \cos(\Omega t) \tag{29}$$

式中

$$\begin{aligned}
a_{s,k} = & -[1/m_k]\int_0^L m\Omega^2 r_x \cos\theta \sin\beta_p \gamma_k \mathrm{d}x - \\
& [1/m_k]\int_0^L m\Omega^2 e_Y \sin\theta \gamma_k \mathrm{d}x + \\
& [1/m_k]\int_0^L (\rho ac/2)\Omega^2 (c/2 + (c/4)\cos\theta - \\
& e_A - e_Y)\beta_p x \gamma_k \mathrm{d}x + [1/m_k]\int_0^L (\rho ac/2)\Omega^2 [(1 - \\
& \beta_p^2)x + 2e_x]x \sin\theta \gamma_k \mathrm{d}x - \\
& [1/m_k]\int_0^L (\rho ac/2)\Omega^2 \cos\theta R r_x d_1 \gamma_k \mathrm{d}x - \\
& \lambda_0 [1/m_k]\int_0^L (\rho ac/2)\Omega^2 \cos\theta R r_x d_3 \gamma_k \mathrm{d}x
\end{aligned}$$

$$\begin{aligned}
c_{k,i} = & [1/m_k]\int_0^L (\rho ac/2)\Omega x \gamma_i \gamma_k \mathrm{d}x - \\
& [1/m_k]\int_0^L (\rho ac/2)\Omega R \sin\theta d_1 \gamma_i \gamma_k \mathrm{d}x - \\
& [1/m_k]\cos(\Omega t)\int_0^L (\rho ac/2)\Omega x \gamma_i \gamma_k \mathrm{d}x - \\
& [1/m_k]\lambda_0 \int_0^L (\rho ac/2)\Omega R \sin\theta d_3 \gamma_i \gamma_k \mathrm{d}x - \\
& [1/m_k]\lambda_0 \cos(\Omega t)\int_0^L (\rho ac/2)\Omega R \sin\theta d_4 \gamma_i \gamma_k \mathrm{d}x
\end{aligned}$$

$$\begin{aligned}
b_{k,ij} = & \int_0^L 2m\Omega \sin\theta \cos\beta_p \int_0^x [\mathrm{d}\gamma_i(y)/\mathrm{d}y] \cdot \\
& [\mathrm{d}\gamma_j(y)/\mathrm{d}y]\mathrm{d}y \cdot \gamma_k(x)\mathrm{d}x
\end{aligned}$$

$$\begin{aligned}
f_k = & -[1/m_k]\int_0^L (\rho ac/2)\Omega^2 \cos\theta R r_x d_2 \gamma_k \mathrm{d}x - \\
& \lambda_0 [1/m_k]\int_0^L (\rho ac/2)\Omega^2 \cos\theta R r_x d_4 \gamma_k \mathrm{d}x
\end{aligned}$$

其中,

$m_k = \int_0^L (m - \rho ac^2/8)\gamma_k^2 \mathrm{d}x$, $r_x = (x + e_x)\cos\beta_p$,

$d_1 = [p(p-1)\sigma a/32](r_x/h_0)^2$,

$d_2 = -(p\sigma a/8)(r_x/h_0)$,

$d_3 = 1 + [p(p-1)/4](r_x/h_0)^2$, $d_4 = -p(r_x/h_0)$

将位移分解成静态位移和动态位移:

$$q_i = q_{si} + q_{di} \tag{30}$$

得静态位移方程:

$$\omega_k^2 q_{sk} = a_{s,k} \tag{31}$$

动态位移方程:

$$\ddot{q}_{dk} + \omega_k^2 q_{dk} = -\sum_{i=1}^{n} c_{k,i}\dot{q}_i - \sum_{1\leqslant i,j\leqslant n} b_{k,ij}(q_{si} + q_{di})\dot{q}_{dj} + f_k \cos(\Omega t) \tag{32}$$

4 实例分析

选用某兆瓦级风力机叶片($NACA63$ 翼型系),各物理参数:$L = 48\mathrm{m}$, $\theta = 2°$, $e_A = 0.25c$, $\beta_P = 5°$, $(e_X, e_Y) = (\cos45°, \sin45°) \times 0.04L$, $\Omega = 15\mathrm{r/min}$, $\rho = 1.25\mathrm{kg/m^3}$, $a = 2\pi$, $n = 4$, $\phi_1 = (x/L)^2$, $\phi_2 = (x/L)^3$, $\phi_3 = (x/L)^4$, $\phi_4 = (x/L)^5$.

表1 两种方法的结果对比

Table 1 comparison of results of two methods

Two Methods	Rayleigh-Ritz method	Error(%)	Finite Element
Primary Frequency(rad/s)	1.6844	1.7	1.7137
Second Frequency(rad/s)	8.4474	4.98	8.8899

表1是两种方法下结果的对比,可见第一阶频率误差较小,第二阶频率误差有所增大.

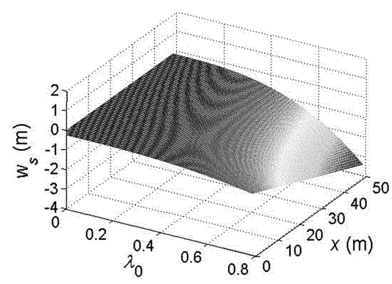

图2 静态位移

Fig. 2 Static displacement

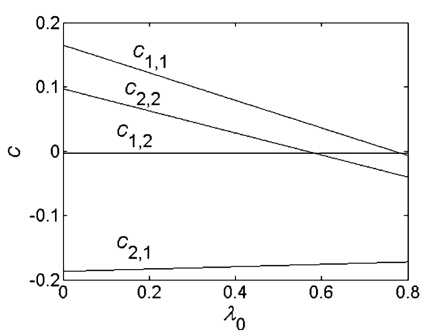

图3 气动阻尼

Fig. 3 Aerodynamic damping

图2是静态位移随入流速度比变化的图像,图像显示:静态位移随入流速度比的增大而增大,越靠近叶尖位移越大,在叶尖处达到最大值.

图3是气动阻尼随入流速度比变化的图像,图像显示:和随入流速度比的增加而减小,当入流速

度比增大到一定程度时,气动阻尼变为负阻尼. 反映模态间耦合的阻尼和随入流速度比的增加而增加,当入流速度比很小时,两阻尼为负值,两模态间相互传递能量.

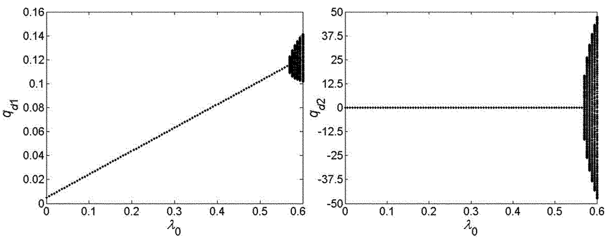

图 4　分岔图

Fig. 4　Bifurcation diagram

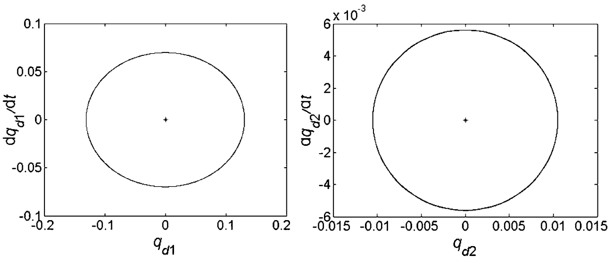

图 5　时的相图

Fig. 5　Phase portrait for

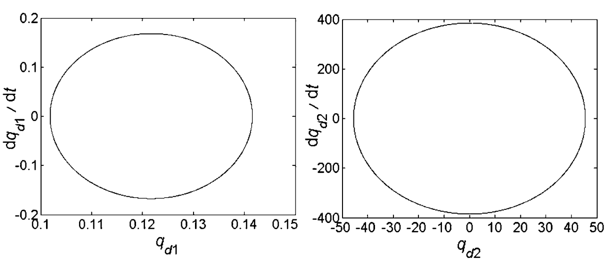

图 6　时的庞加莱映射

Fig. 6　Poincaré map for

图 4 是对应于前两阶模态的动态位移分叉图,图 5 是入流速度比为 0.1 时的相图,图 6 是入流速度比 0.6 是的庞加莱映射. 图像显示:当入流速度比较小时,运动为小振幅的周期运动,随着入流速度比的增大,运动变为大振幅的拟周期运动.

5　结论

本文研究了风力机叶片大挠度挥舞振动特性,使用哈密顿原理建立了控制方程,采用瑞利 - 利兹法计算了频率和模态函数,使用分岔图、相图和庞加莱映射等非线性动力学工具分析了振动响应,得到如下结论:挥舞振动静态位移随入流速度比的增大而增大,越靠近叶尖位置静态位移越大;当入流速度比较小时,振动为小振幅的周期运动,入流速度比较大时,振动为大振幅的拟周期运动.

参　考　文　献

1　李本立,宋宪耕,贺德馨,安玉华. 风力机结构动力学. 北京: 北京航空航天大学出版社, 1999:28 ~ 123 (Li B L, Song X G, He D X, An Y H. Structure dynamic analysis of wind turbine. Beijing: Beijing aerospace university press, 1999:28 ~ 123 (in Chinese))

2　Z L Mahri. Fatigue estimation of a rotating blade. Word renewable energy congress, Perth, Australia, 1999,36 ~ 78

3　Z L Mahri. Fatigue estimation for a rotating blade of a wind turbine. *Revue des energie renouvelable UNESCO-CDER*, 2002,5 :39 ~ 47

4　Z L Mahri, M S Rouabah. Calculation of dynamic stresses using finite element method and prediction of fatigue failure for wind turbine rotor. *Wseas transactions on applied and theoretical mechanics*, 2008,1(3):28 ~ 41

5　O Song, L Librescu. Modeling and dynamic behavior of rotating blades carrying a tip mass and incorporating adaptive capabilities. *Acta Mechanica*, 1999 (134): 169 ~ 197

6　韩新月,申新贺,陈研,吴涛. 科氏力对水平轴风力机叶片的影响. 能源工程 2008,(3): 8 ~ 11 (Han X Y, Shen X H, Chen Y, Wu T. The influence of Coriolis force on the horizontal axis wind turbine blade. *Energy Engineering*, 2008, (3):8 ~ 11(in Chinese))

7　吕计男,刘子强. NREL S809 风力机叶片动力学特征分析. 第十一届全国空气弹性学术交流会, 云南丽江, 2009: 579 ~ 584 (Lv J N, Liu Z Q. Characteristic analysis of dynamics of blades of NREL S809 wind turbines. The 11th national academic exchanges of air elasticity. Yun nan Li jiang, 2009: 579 ~ 584(in Chinese))

8　王建礼,赵晓路,廖猜猜,石可重,徐建中. 风力机叶片固有频率优化设计研究. 工程热物理学报, 2010, 31 (11):1843 ~ 1846 (Wang J L, Zao X L, Liao C C, Shi K Z, Xu J Z. Study on the optimization design of wind turbine blade natural frequency. *Journal of Engineering Thermophysics*, 2010, 31(11):1843 ~ 1846(in Chinese))

9　梁明轩,陈长征,风力机叶片流固耦合效应研究. 振动与冲击, 2010, 29(S):130 ~ 132 (Liang M X, Chen C Z, Study on Fluid. Structure Interaction of Wind Turbine Blade. *Journal of Vibration and Shock*, 2010, 29(S):130 ~ 132(in Chinese))

10　Li J , Chen J Y, Chen X B. Dynamic characteristics analysis of the offshore wind turbine blades. *Journal of Marine Science and Application*, 2011,10: 82 ~ 87

11 J W Larsen, S R K Nielsen. Non-linear dynamics of wind turbine wings. *International Journal of Non-linear Mechanics*, 2006,41 :629 ~ 643

12 J W Larsen, S R K Nielsen. Nonlinear parametric instability of wind turbine wings. *Journal of Sound and Vibration*, 2007, 299: 64 ~ 82

13 J W Larsen, R Iwankiewicz, S R K Nielsen. Nonlinear stochastic stability analysis of wind turbine wings by Monte Carlo simulations. *Probabilistic Engineering Mechanics*, 2007,22 :181 ~ 193

FLAPWISE CHARACTERISTICS OF A WIND TURBINE BLADE WITH LARGE DEFLECTION *

Liu Qikuan[1,3] Li Liang[2] Zhang Zhijun[3] Li Yinghui[2]

(1. *Department of Mathematics KunMing University*, *Kunming* 650214, *China*)

(2. *School of Mechanics and Engineering Southwest Jiao tong University*, *Chengdu* 610031, *China*)

(3. *College of Mathematics Chengdu University of Information Technology*, *Chengdu* 610225, *China*)

Abstract The characteristics of flap vibration of a wind turbine blade with large deflection were studied. The governing equation of the vibration under unsteady aerodynamic loads, whose expressions were derived from the Greenberg expressions, was established by applying the Hamiltonian principle. The Rayleigh-Ritz method was used to calculate frequencies and mode functions. Based on these mode functions, the partial differential equation governing the vibration was discreted by using the Galerkin's method. The displacement was resolved to static displacement and dynamic displacement, and the equations of the static and dynamic displacement were obtained. The effects of the inflow ration to the static displacement and the aerodynamic damping were discussed. The dynamic response was analyzed by using the nonlinear-dynamical tools. The results show: 1) that the static displacement rises with the inflow ratio, and it reaches the limit at the blade tip; 2) that the vibration is a harmonic motion for small inflow ratio, and it becomes a quasi-harmonic motion when the inflow ratio is big.

Key words wind turbine blade, large deflection, flap vibration

Received 9 October 2011, revised 14 February 2012.

* The project supported by National Natural Science Foundation of China (11072204), Basic Research in Application Program of Sichuan (2010JY0079) and Introduction Talents in Research Project of Kunming University (YJL12005)